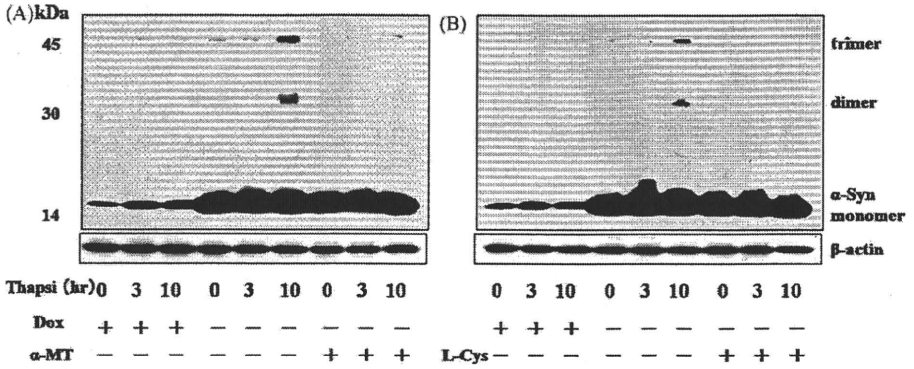

Fig. 3. An analysis of α-syn oligomerization in response to thapsigargin. Neural differentiated cells were incubated for 3 days either under induced or repressed conditions. After 3 days of induction of α-syn, cells are exposed to 300 nM thapsigargin for 0, 3 and 10 h. Cell lysates were analyzed by Western blotting with anti-α-syn antibody. A representative Western blot analysis reveals the increase of α-syn oligomers 10 h after 300 nM thapsigargin exposure. Additional α-MT (100 μM) and L-cysteine (10 μM) both decrease the oligomerization which is caused by thapsigargin.

(39.2%, 25.8%, 22.7%, 9.0% decrease, respectively). A significant decrease was observed in the number of apoptotic cells following α-MT treatment in response to thapsigargin and tunicamycin exposure (<0.05). These data suggest that α-syn enhances cell vulnerability to stressors. In particular, endogenous CA metabolites lead to further enhancement of cell vulnerability to ER stressors.

3.3. *Thapsigargin enhanced α-syn oligomerization in a presence of CA*

The kinetics of α-syn following thapsigargin exposure were investigated. Thapsigargin increased oligomers of α-syn in α-syn overexpressed conditions. However, the inhibition of CA by α-MT decreased the oligomerization of α-syn (Fig. 3A). Moreover, L-cysteine, a scavenger of *o*-quinone, also decreased the oligomerization of α-syn (Fig. 3B). These findings suggest that endogenous CA and CA-related quinones are responsible for the observed increase in α-syn oligomers.

3.4. *Overexpression of α-syn suppresses UPR to thapsigargin*

The molecular behavior of the major three branches of the UPR, governed by the ER stress sensors IRE1α, PERK-eIF2α, and ATF6α, respectively, were investigated to evaluate the influence of α-syn on the ER. Protein levels of nuclear ATF6α p50 (nATF6α p50) were increased 1.5 h after thapsigargin exposure in α-syn repressed conditions (136% relative increase). However, nATF6α p50 showed a 62% relative increase under α-syn induced conditions (Fig. 4A). IRE1α was immunoprecipitated to determine whether there was any serine-phosphorylation of IRE1α in order to identify the activation of the IRE1α-related pathway. An increased level of phosphorylation of IRE1α was observed at 1.5 h

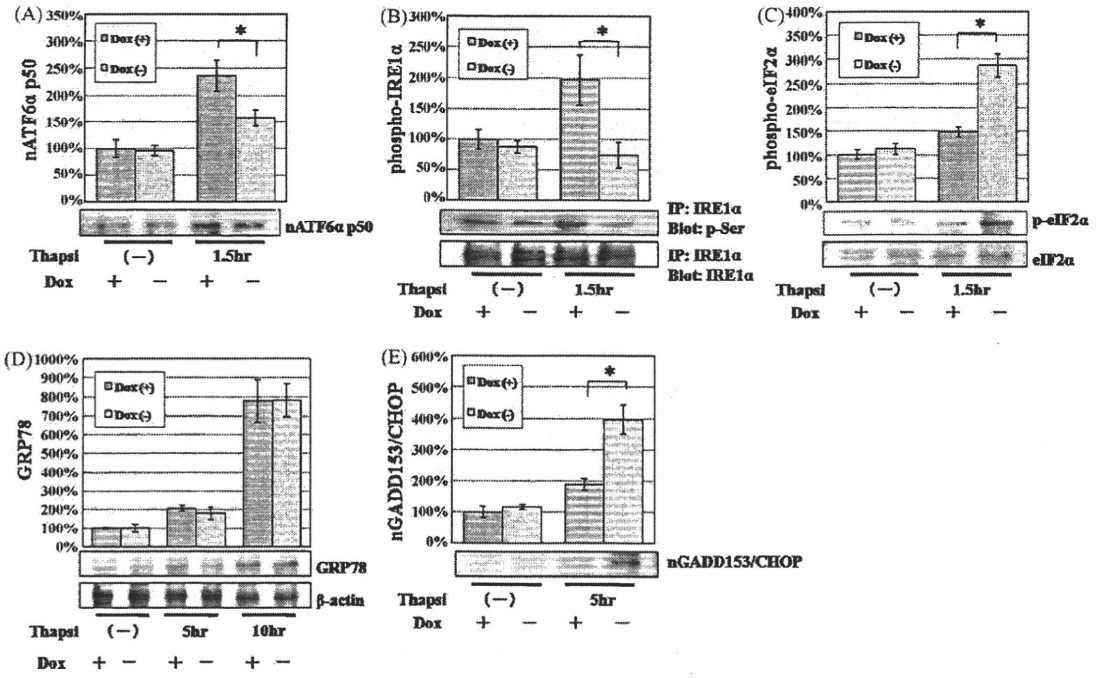

Fig. 4. An analysis of the unfolded protein response to thapsigargin. Differentiated PC12 cells were incubated for 3 days either under induced or repressed conditions. After 3 days, cells were exposed to 300 nM thapsigargin for 0, 1.5, 5 and 10 h. IRE1α were immunoprecipitated and analyzed on a Western blot with phosphoserine antibody then with an antibody that recognizes total IRE1α. Each histogram shows the semi-quantification data of the protein levels ($N = 4$). The Western blot analysis reveals a decrease of nATF6α p50 induction (A) and phosphorylation of IRE1α (B) under α-syn expressing conditions. No significant difference is observed in the induction of GRP78 (D). However, increases of both eIF2α phosphorylation and nGADD153/CHOP induction are observed (C and E). Data are presented as the mean ± SD. $^{*}P < 0.05$.

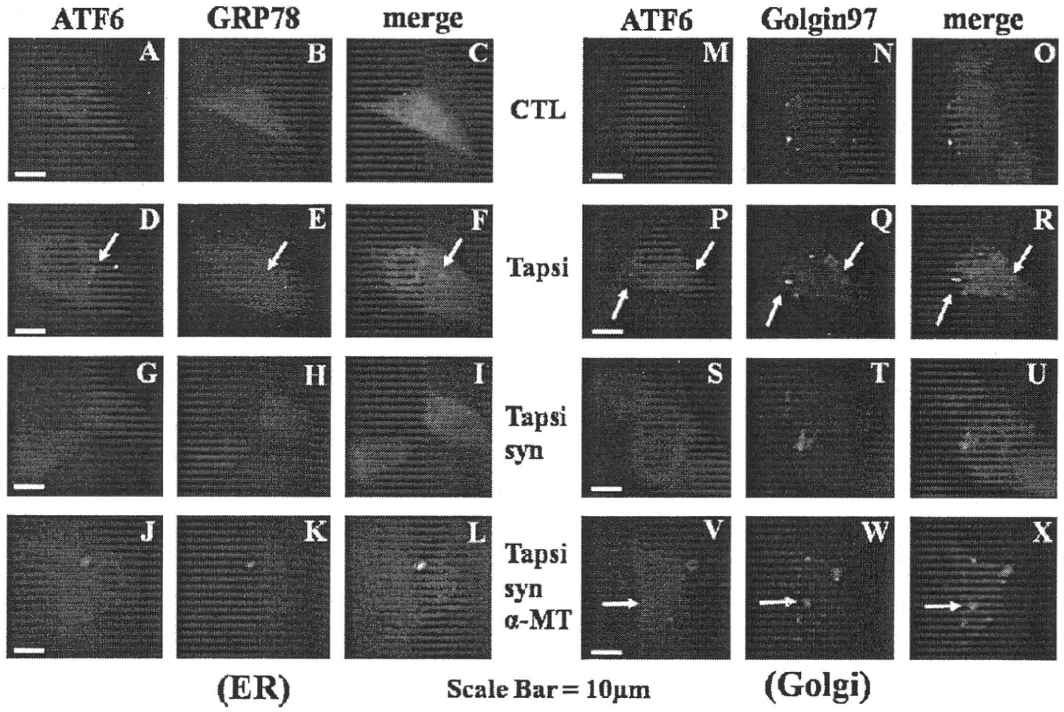

Fig. 5. Inhibition of ATF6α trafficking to the Golgi apparatus by α-syn overexpression. Neural differentiated cells were prepared in 8-well chamber slides (3 days induction). ATF6α shows red fluorescence. Golgin97, a marker of Golgi apparatus, and GRP78, a marker of ER show green fluorescence. Under untreated conditions (CTL), ATF6α is co-located with GRP78 (A–C), but not with Gogin97 (M–O). However, ATF6α co-locating with Goligin97 is observed 3 h after exposure to 300 nM thapsigargin (P–R). Under α-syn expressing conditions, the transfer of ATF6α to Golgi apparatus is decreased (S–U). Additional α-MT (100 μM) increases ATF6α co-locating with Goligin97 (V–X). The scale bar represents 10 μm (For interpretation of the references to color in this figure legend, the reader is referred to the web version of the article).

after thapsigargin treatment (97% relative increase). However, the phosphorylation of IRE1α was repressed by α-syn overexpression (Fig. 4B). On the other hand, an increased level of phosphorylation of eIF2α was observed at 1.5 h after thapsigargin treatment under α-syn induced conditions (175% relative increase; Fig. 4C). Thapsigargin increased the expression level of GRP78, an ER chaperone that is vital for ER-stress induced UPR resolution (Fig. 4D). However, no significant

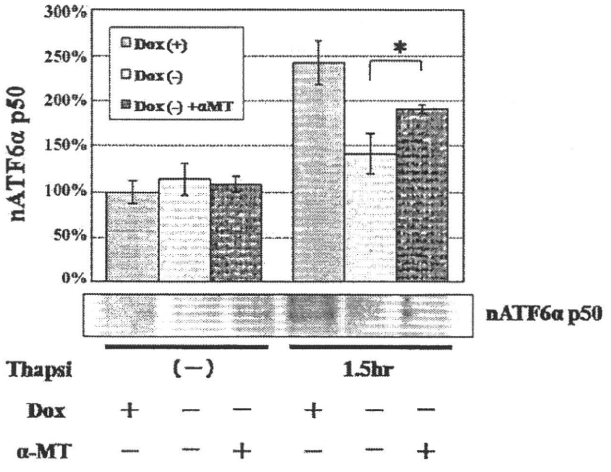

Fig. 6. Inhibition of endogenous CA prevents the reduction of nATF6α p50. Differentiated PC12 cells were incubated for 3 days in either induced or repressed conditions. The cells are exposed to 300 nM thapsigargin for 1.5 h. The histogram shows the semi-quantification data of the nATF6α p50 protein levels ($N = 4$). Additional α-MT (100 μM) prevents the reduction of nATF6α p50 caused by α-syn expression. Data are presented as the mean ± SD. $^{*}P < 0.05$.

difference was observed between the repressed and induced conditions. Nuclear GADD153/CHOP (nGADD153/CHOP), a transcription factor that can induce apoptosis, showed a higher protein levels in α-syn overexpressed conditions (282% relative increase) in comparison to repressed conditions (89% relative increase) 5 h after thapsigargin treatment (Fig. 4E). GRP78 and nGADD153/CHOP protein levels were measured under the same conditions using human β-syn overexpressing cells in order to investigate whether only an overexpression of protein influence UPR. Both GRP78 and nGADD153/CHOP did not show significant differences between the repressed and induced conditions (Supplementary data). Immunofluorescent staining suggested that the transfer of ATF6α to the Golgi apparatus was inhibited by the overexpression of α-syn (Fig. 5A–I, M–U).

3.5. Inhibition of CA metabolism rescues the ATF6α inactivation caused by α-syn overexpression

Finally, the relationship between endogenous CA and the dysfunction of the ATF6α pathway was investigated. Lower protein levels of nATF6α p50 were observed in response to thapsigargin under α-syn induced conditions (42% relative decrease) in comparison to repressed conditions (Fig. 6). However, the administration 100 μM α-MT reduced the inhibition of nATF6α p50 induction under α-syn overexpressed conditions (21% relative decrease). Moreover, immunofluorescent staining suggested that the inhibited transfer of ATF6α to the Golgi apparatus was partially improved by α-MT under α-syn overexpressing conditions (Fig. 5J–L, V–X). These results suggest that endogenous CA enhances the impairment in ER-Golgi trafficking caused by the overexpression of human α-syn.

4. Discussion

Recent findings suggest that oligomers, rather than the fibrillar amyloid deposits of α-syn, represent the principal toxic species in PD (Kayed et al., 2004). *In vitro* studies have also demonstrated that CA stabilizes the protofibrillar form of α-syn, thus forming a CA-α-syn adduct (Conway et al., 2001). Therefore, the oligomerization of α-syn may interact with CA in the pathogenesis of PD. On the other hand, environmental stressors have been used as a PD model both *in vitro* and in animals. Although dysfunctions of mitochondria, ER and ubiquitin-proteasome have been implicated in α-syn pathogenesis (Mizuno et al., 2008), there is still insufficient evidence to determine whether CA is involved in these processes. A previous report demonstrated that L-DOPA and dopamine enhance the formation of aggregates under proteasome inhibition in PC12 cells (Yoshimoto et al., 2005). However, the amount of rat α-syn in PC12 cells is so small that it is not easy to evaluate the formation of oligomers and aggregates without proteasome inhibition. Therefore, the current study employed the overexpression of human α-syn in PC12 cells.

An increase in apoptotic cell death was observed over a 7-day incubation period, followed by an increase in the expression of human α-syn. These cells were also vulnerable to ER stress and mitochondrial toxicities at an earlier incubation stage for 3 days (Figs. 1C and 2B). These findings indicate that an overexpression of human α-syn is harmful in this cell line. Interestingly, WT α-syn overexpressing models of PD often fail to reproduce the cardinal features of the disease (Giasson et al., 2002; Lee et al., 2002). On the other hand, only an overexpression of human WT α-syn induces acute cell death in some neural-differentiated forms of human embryonic cells differentiated into neuroepithelial cells (Schneider et al., 2007). This suggests that the cell line in the current study is a suitable model to investigate the association between CA and the pathogenesis of PD.

Reduced apoptosis by α-MT also suggests that CA enhances α-syn toxicities (Figs. 1D and 2B). The neurotoxicity of CA-quinone formed by auto-oxidation of CA is associated with dopaminergic neuron-specific oxidative stress (Miyazaki et al., 2006). Although CA-quinone is a reactive metabolite that preferentially binds to reduced cysteine residues within polypeptides, it also binds covalently to α-syn which has no cysteine residue (Conway et al., 2001; LaVoie et al., 2005). Since not only α-MT but also L-cysteine inhibited an increase of α-syn oligomers which were induced by thapsigargin administration (Fig. 3), CA-quinone formation might be involved in the pathogenesis of PD. The observed α-syn oligomerization in response to thapsigargin was not associated with serine 129 phosphorylation of α-syn (*data not shown*). Therefore, CA-quinone may directly interact with α-syn protein and thereby cause a conformational change. Thapsigargin is an inhibitor of the Ca^{2+} pump in the ER membrane. Therefore, the disequilibrium of cytosolic Ca^{2+} probably causes oxidative stress, thus resulting in the enhancement of CA oxidation and the increase of toxic oligomers.

Since thapsigargin enhanced α-syn cytotoxicity associated with CA, the UPR in ER was investigated. In mammals, three signaling pathways operate for the UPR, the IRE1-XBP1, PERK-eIF2α, and ATF6α pathways (Schröder and Kaufman, 2005). In the present study, thapsigargin activated eIF2α phosphorylation and nGADD153/CHOP induction in α-syn overexpressed conditions. However, the protein levels of ATF6α p50 and IRE1α phosphorylation decreased as a response to thapsigargin (Fig. 4). The inhibition of the CA metabolism therefore rescued the ATF6α pathway dysfunction (Figs. 5 and 6). ATF6α makes an initial response before the IRE1α and PERK-eIF2α pathways in mammals, and the signal transfer via ER-Golgi trafficking is unique to ATF6α in the three signal branches of UPR (Chen et al., 2002). Therefore, the impairment of the ATF6α and IRE1α pathways induced by CA-quinone might cause an earlier breakdown of UPR. The phosphorylation of eIF2α has been reported to increase in human autopsy brain specimens obtained from PD patients (Hoozemans et al., 2007). These observations also support the current experimental findings.

Acknowledgments

This work was supported in part by Grants-in-Aid for Scientific Research from the Ministry of Education, Culture, Sports, Science and Technology of Japan (Nakaso), the Research Committee on Neurodegenerative Diseases, Ministry of Health, Labor and Welfare, Japan (Nakashima), and the Venture Business Laboratory, Tottori University (Ito).

Appendix A. Supplementary data

Supplementary data associated with this article can be found, in the online version, at doi:10.1016/j.neures.2009.10.005.

References

Auluck, P.K., Chan, H.Y., Trojanowski, J.Q., Lee, V.M., Bonini, N.M., 2002. Chaperone suppression of alpha-synuclein toxicity in a Drosophila model for Parkinson's disease. Science 295, 865–868.

Schneider, Bernard, L., Seehus, Corey R., Capowski, Elizabeth E., Aebischer, Patrick, Zhang1, Su-Chun, Svendsen, Clive N., 2007. Over-expression of alpha-synuclein in human neural progenitors leads to specific changes in fate and differentiation. Hum. Mol. Genet. 16, 651–666.

Cao, S., Gelwix, C.C., Caldwell, K.A., Caldwell, G.A., 2005. Torsin-mediated protection from cellular stress in the dopaminergic neurons of *Caenorhabditis elegans*. J. Neurosci. 25, 3801–3812.

Chartier-Harlin, M.C., Kachergus, J., Roumier, C., Mouroux, V., Douay, X., Lincoln, S., Levecque, C., Larvor, L., Andrieux, J., Hulihan, M., Waucquier, N., Defebvre, L., Amouyel, P., Farrer, M., Destée, A., 2004. Alpha-synuclein locus duplication as a cause of familial Parkinson's disease. Lancet 364, 1167–1169.

Chen, X., Shen, J., Prywes, R., 2002. The luminal domain of ATF6 senses endoplasmic reticulum (ER) stress and causes translocation of ATF6 from the ER to the Golgi. J. Biol. Chem. 277, 13045–13052.

Conway, K.A., Rochet, J.C., Bieganski, R.M., Lansbury Jr., P.T., 2001. Kinetic stabilization of the alpha-synuclein protofibril by a dopamine-alpha-synuclein adduct. Science 294, 1346–1349.

Cooper, A.A., Gitler, A.D., Cashikar, A., Haynes, C.M., Hill, K.J., Bhullar, B., Liu, K., Xu, K., Strathearn, K.E., Liu, F., Cao, S., Caldwell, K.A., Caldwell, G.A., Marsischky, G., Kolodner, R.D., Labaer, J., Rochet, J.C., Bonini, N.M., Lindquist, S., 2006. α-synuclein blocks ER-golgi traffic and Rab1 rescues neuron loss in Parkinson's models. Science 21, 324–328.

Giasson, B.I., Duda, J.E., Quinn, S.M., Zhang, B., Trojanowski, J.Q., Lee, V.M., 2002. Neuronal alpha-synucleinopathy with severe movement disorder in mice expressing A53T human alpha-synuclein. Neuron 34, 521–533.

Holtz, W.A., O'Malley, K.L., 2003. Parkinsonian mimetics induce aspects of unfolded protein response in death of dopaminergic neurons. J. Biol. Chem. 278, 19367–19377.

Hoozemans, J.J., van Haastert, E.S., Scheper, W., 2007. Activation of the unfolded protein response in Parkinson's disease. Biochem. Biophys. Res. Commun. 354, 707–711.

Hsu, L.J., Sagara, Y., Arroyo, A., Rockenstein, E., Sisk, A., Mallory, M., Wong, J., Takenouchi, T., Hashimoto, M., Masliah, E., 2000. Alpha-synuclein promotes mitochondrial deficit and oxidative stress. Am. J. Pathol. 157, 401–410.

Ibáñez, P., Bonnet, A.M., Débarges, B., Lohmann, E., Tison, F., Pollak, P., Agid, Y., Dürr, A., Brice, A., 2004. Causal relation between alpha-synuclein gene duplication and familial Parkinson's disease. Lancet 364, 1169–1171.

Imai, Y., Soda, M., Inoue, H., Hattori, N., Mizuno, Y., Takahashi, R., 2001. An unfolded putative transmembrane polypeptide, which can lead to endoplasmic reticulum stress, is a substrate of Parkin. Cell 105, 891–902.

Imai, Y., Soda, M., Hatakeyama, S., Akagi, T., Hashikawa, T., Nakayama, K.I., Takahashi, R., 2002. CHIP is associated with Parkin, a gene responsible for familial Parkinson's disease, and enhances its ubiquitin ligase activity. Mol. Cell 10, 55–67.

Kayed, R., Sokolov, Y., Edmonds, B., McIntire, T.M., Milton, S.C., Hall, J.E., Glabe, C.G., 2004. Permeabilization of lipid bilayers is a common conformation-dependent activity of soluble amyloid oligomers in protein misfolding diseases. J. Biol. Chem. 279, 46363–46366.

LaVoie, M.J., Ostaszewski, B.L., Weihofen, A., Schlossmacher, M.G., Selkoe, D.J., 2005. Dopamine covalently modifies and functionally inactivates parkin. Nat. Med. 11, 1159–1161.

Lee, M.K., Stirling, W., Xu, Y., Xu, X., Qui, D., Mandir, A.S., Dawson, T.M., Copeland, N.G., Jenkins, N.A., Price, D.L., 2002. Human alpha-synuclein-harboring familial Parkinson's disease-linked Ala-53 → Thr mutation causes neurodegenerative disease with alpha-synuclein aggregation in transgenic mice. Proc. Natl. Acad. Sci. U.S.A. 99, 8968–8973.

Lo Bianco, C., Ridet, J.L., Schneider, B.L., Deglon, N., Aebischer, P., 2002. Alpha-Synucleinopathy and selective dopaminergic neuron loss in a rat lentiviral-based model of Parkinson's disease. Proc. Natl. Acad. Sci. U.S.A. 99, 10813–10818.

Masliah, E., Rockenstein, E., Veinbergs, I., Mallory, M., Hashimoto, M., Takeda, A., Sagara, Y., Sisk, A., Mucke, L., 2000. Dopaminergic loss and inclusion body formation in alpha-synuclein mice: implications for neurodegenerative disorders. Science 287, 1265–1269.

Miyazaki, I., Asanuma, M., Diaz-Corrales, F.J., Fukuda, M., Kitaichi, K., Miyoshi, K., Ogawa, N., 2006. Methamphetamine-induced dopaminergic neurotoxicity is regulated by quinone-formation-related molecules. FASEB J. 20, 571–573.

Mizuno, Y., Hattori, N., Kubo, S., Sato, S., Nishioka, K., Hatano, T., Tomiyama, H., Funayama, M., Machida, Y., Mochizuki, H., 2008. Progress in the pathogenesis and genetics of Parkinson's disease. Philos. Trans. R. Soc. Lond. B. Biol. Sci. 363, 2215–2227.

Prasad, J.E., Kumar, B., Andreatta, C., Nahreini, P., Hanson, A.J., Yan, X.D., Prasad, K.N., 2004. Overexpression of alpha-synuclein decreased viability and enhanced sensitivity to prostaglandin E(2), hydrogen peroxide, and a nitric oxide donor in differentiated neuroblastoma cells. J. Neurosci. Res. 76, 415–422.

Ryu, E.J., Harding, H.P., Angelastro, J.M., Vitolo, O.V., Ron, D., Greene, L.A., 2002. Endoplasmic reticulum stress and the unfolded protein response in cellular models of Parkinson's disease. J. Neurosci. 22, 10690–10698.

Schröder, M., Kaufman, R.J., 2005. ER stress and the unfolded protein response. Mutat. Res. 569, 29–63.

Singleton, A.B., Farrer, M., Johnson, J., Singleton, A., Hague, S., Kachergus, J., Hulihan, M., Peuralinna, T., Dutra, A., Nussbaum, R., Lincoln, S., Crawley, A., Hanson, M., Maraganore, D., Adler, C., Cookson, M.R., Muenter, M., Baptista, M., Miller, D., Blancato, J., Hardy, J., Gwinn-Hardy, K., 2003. Alpha-synuclein locus triplication causes Parkinson's disease. Science 302, 841.

Spillantini, M.G., Crowther, R.A., Jakes, R., Hasegawa, M., Goedert, M., 1998. α-Synuclein in filamentous inclusions of Lewy bodies from Parkinson's disease and dementia with Lewy bodies. Proc. Natl. Acad. Sci. U.S.A. 95, 6469–6473.

Sugeno, N., Takeda, A., Hasegawa, T., Kobayashi, M., Kikuchi, A., Mori, F., Wakabayashi, K., Itoyama, Y., 2008. Serine 129 phosphorylation of α-synuclein induces unfolded protein response-mediated cell death. J. Biol. Chem. 283, 23179–23188.

Xu, J., Kao, S.Y., Lee, F.J., Song, W., Jin, L.W., Yankner, B.A., 2002. Dopamine-dependent neurotoxicity of alpha-synuclein: a mechanism for selective neurodegeneration in Parkinson disease. Nat. Med. 8, 600–606.

Yoshimoto, Y., Nakaso, K., Nakashima, K., 2005. L-dopa and dopamine enhance the formation of aggregates under proteasome inhibition in PC12 cells. FEBS Lett. 579, 1197–1202.

Parkinsonism and Related Disorders xxx (2010) 1–3

Contents lists available at ScienceDirect

Parkinsonism and Related Disorders

journal homepage: www.elsevier.com/locate/parkreldis

Short communication

Relationship between ^{123}I-MIBG scintigrams and REM sleep behavior disorder in Parkinson's disease☆

Takashi Nomura [a,*], Yuichi Inoue [b,c], Birgit Högl [d], Yusuke Uemura [a], Michio Kitayama [a], Takashi Abe [b], Hidenao Miyoshi [e], Kenji Nakashima [a]

[a] Division of Neurology, Department of Brain and Neurosciences, Faculty of Medicine, Tottori University, Japan
[b] Japan Somnology Center, Neuropsychiatric Research Institute, Japan
[c] Department of Somnology, Tokyo Medical University, Japan
[d] Department of Neurology, Innsbruck Medical University, Austria
[e] Department of Radiology, Faculty of Medicine, Tottori University, Japan

ARTICLE INFO

Article history:
Received 26 March 2010
Received in revised form
14 July 2010
Accepted 14 August 2010

Keywords:
RBD symptoms
MIBG scintigrams
Parkinson's disease
RWA

ABSTRACT

Background: Uptake of ^{123}I-labeled meta-iodobenzylguanidine (MIBG) in myocardial scintigrams has been shown to be as low in patients with idiopathic RBD as in Parkinson's disease (PD) patients.
Aim for study: To clarify whether the existence of RBD accelerates autonomic dysfunction in PD, we investigated the association between MIBG scintigraphic findings and RBD measures among non-dementia PD patients.
Subjects & methods: We conducted clinical interviews to assess REM sleep behavior disorder (RBD) symptoms, and performed polysomnograms (PSG) recordings and MIBG scintigrams on 49 PD patients. The patients were divided into three groups (PD with clinical RBD, PD with subclinical RBD, and PD with normal REM sleep).
Results: PD patients with clinical RBD had reduced MIBG uptake as determined by heart-to-mediastinum ratios of the delayed image compared to those with subclinical RBD and those with normal REM sleep. Multiple linear regression analysis revealed that only the existence of RBD symptoms was significantly associated with reduced MIBG uptake among PD patients without dementia after adjusting for demographic and PD symptom-related variables.
Conclusion: PD patients with clinical RBD might suffer from a wider α-synuclein pathology, including reduced cardiac sympathetic ganglia function as reflected by a lowered MIBG uptake.

1. Introduction

REM sleep behavior disorder (RBD) is characterized by vigorous and injurious behaviors related to vivid, action-filled, and violent dreams in nocturnal REM sleep. RBD is diagnosed when a patient has both violent dream enactment behavior and REM sleep without atonia (RWA) on polysomnograms (PSG). RBD has been widely accepted as one of the important co-morbidities of PD [1] and has been proposed to be one of the risk factors for developing hallucinations [2] [3] in PD patients. Moreover, orthostatic abnormalities were found to be more frequent in PD patients having RBD compared to those without these symptoms [3].

Cardiac uptake of ^{123}I-labeled meta-iodobenzylguanidine (MIBG) on scintigrams is known to be reduced in PD patients [4]. Notably, reduced MIBG uptake on scintigrams in patients with idiopathic RBD is quite similar to that of PD patients [5]. However, it has not been determined whether reductions in MIBG uptake are lower in PD patients with RBD versus those without RBD. To clarify this issue, we investigated the association between MIBG scintigraphic findings and RBD measures among PD patients.

2. Methods

This study was approved by the ethics committees of Tottori University, and all patients gave informed consent to take part in it. Patients with PD who had been hospitalized in the Department of Neurology at the University Hospital from July 2004 to June 2008 were targeted for this study, and forty-nine PD patients agreed to participate. The mean follow-up period on the subject patients was 6.3 ± 5.1 years. They had been receiving oral dopaminergic agents [levodopa dose equivalents

☆ The review of this paper was entirely handled by an Associate Editor, Eng-King Tan.

* Corresponding author. Division of Neurology, Department of Brain and Neurosciences, Faculty of Medicine, Tottori University, 36-1 Nishicho, Yonago 683-8504, Japan. Tel.: +81 859 38 6757; fax: +81 859 38 6759.
E-mail address: ntnomura@med.tottori-u.ac.jp (T. Nomura).

1353-8020/$ – see front matter
doi:10.1016/j.parkreldis.2010.08.011

(LDEs) [6] PD: 371 ± 214 mg/day]. We excluded patients from this study who were taking selegiline or antidepressants and those having suffered from heart failure and/or diabetes mellitus since these factors might have affected the MIBG scintigraphic findings.

Overnight PSG recordings were performed by standardized methods [6]. During REM stage sleep, submental phasic EMG activity (defined as 3-s mini-epochs containing phasic twitches which are at least four times higher than the background EMG activity) or submental tonic EMG activity with durations of more than half of a 30-s epoch was scored as RWA [7].

All the PD patients and their bed partners were also systematically interviewed regarding their sleep problems by a physician specializing in sleep disorders. Interviews especially focused on dream enactment behavior or vocalization while dreaming within one month before the PSG. In line with criteria from the second edition of the International Classification of Sleep Disorders [1], we diagnosed clinical RBD when a patient had both RWA on PSG and the experience of dream enactment behaviors associated with uncomfortable dream content during the preceding year, and included not only violent cases but also non-violent cases. This last criterion was included according to the suggestion by Oudiette et al. [8] that non-violent symptoms might represent the first step in the neurodegenerative process of the disorder. We also defined patients with RWA but without RBD symptoms as subclinical RBD. Finally, we categorized the patients into three groups: PD group with clinical RBD, PD group with subclinical RBD, and PD group with normal REM sleep.

Patients received an intravenous injection of 111-mBq of ^{123}I-MIBG (Daiichi Radioisotope Laboratories, Tokyo, Japan). A single photon emission computed tomography (SPECT) image was obtained in an anterior view after 30 min for the early image and after 3.5 h for the delayed one. Average counts per pixel in the heart and mediastinum were used to calculate the heart-to-mediastinum (H/M) ratio. In this study, the H/M ratio of the delayed images, which display the neuronal uptake of MIBG scintigrams more explicitly than those of the early image [9], were used for the analysis.

We compared the continuous variables, including MIBG scintigraphic findings, among the above three groups by using an analysis of variance (ANOVA) followed by *post hoc* testing with Bonferroni correlation. A χ^2-test was also used to compare the categorical variables. Finally, multiple linear regression analysis was performed to explore the risk model of reduced MIBG uptake among the PD patients. The independent variables included age, gender, PD symptom-related variables (duration of morbidity, Hoehn & Yahr stages, and LDEs), and RBD measures (RBD symptoms and RWA on PSGs). Statistical significance was defined as $p < 0.05$ (SPSS, ver. 15.0J, SPSS Japan, 2006).

3. Results

Twenty-six of the 49 PD patients without dementia had RWA on PSG (53.1%); 18 patients were classified as having clinical RBD (36.7%), including 8 with violent behavior and 10 with non-violent behavior. Eight patients were classified as displaying subclinical RBD (16.3%). The other 23 patients had normal REM sleep (46.9%). There were no significant differences in any of the above descriptive parameters among the three PD groups (Table 1).

There was a significant difference in H/M ratios on the MIBG scintigrams among the three groups [$F_{3,54} = 6.33$, $p = 0.001$]. *Post hoc* tests revealed that the PD group with clinical RBD had significantly lower values compared to both the group with subclinical RBD ($p < 0.01$) and the group with normal REM sleep ($p < 0.01$). However, there were no significant differences in H/M ratios between the PD group with subclinical RBD and the group with normal REM sleep (Fig. 1). Within the PD group exhibiting clinical RBD, there was no significant difference in the ratio between patients with violent behavior and those with non-violent behavior (patients with violent behavior: 1.18 ± 0.24, those with non-violent behavior: 1.16 ± 0.09).

Multiple linear regression analysis revealed that the existence of RBD ($\beta = -0.511$, $p = 0.002$) appeared to be the only significantly associated factor among the studied independent variables for reduced MIBG uptake in the final model ($R^2 = 0.314$, $p = 0.006$; Table 2).

4. Discussion

Our results confirmed that MIBG uptake is decreased in non-dementia PD patients with clinical RBD. Moreover, among the studied variables, the existence of RBD symptoms alone was associated with reduced MIBG uptake among PD patients. Interestingly, our results indicate that patients with subclinical RBD do not show significantly reduced MIBG uptake. This finding raises the possibility that neuronal loss and inclusion of Lewy bodies in the sympathetic ganglia as reflected by the reduced MIBG uptake is marked, especially in PD patients having clinical RBD symptoms. PD patients experiencing hallucinations are likely to have more reduced MIBG uptake compared to those that do not [10]. Therefore, our results may corroborate the idea that the existence of RBD symptoms in PD is one of the risk factors for developing hallucinations [2].

As mentioned above, patients with idiopathic RBD have reduced MIBG uptake [5]. Moreover, they have been characterized as likely to have autonomic symptoms including orthostatic hypotension [3] and cardiac dysfunction during both wakefulness and sleep [11,12]. As for PD patients, orthostatic abnormalities have been reported to be more frequent in patients with RBD [3]. Taking this finding and the present MIBG results together, it is possible that the existence of RBD symptoms accelerates autonomic dysfunction in PD patients. Considering that patients with non-violent behaviors showed MIBG findings similar to those with violent behaviors in the present study, it appears that the existence (but not the severity) of RBD symptoms might be related with reduced MIBG uptake. From this finding, we speculate that patients with α-synuclein pathology expanding into the limbic system, resulting in the occurrence of uncomfortable dreams associated with RBD symptoms, might simultaneously have lesions of cardiac sympathetic ganglia.

Our study has several limitations. First, our study did not include normal age-matched control subjects or patients with idiopathic RBD. Although our results show a clear difference in MIBG uptake between PD patients with and without clinical RBD, further study including these two control groups is necessary for drawing definitive conclusions. Second, the existence of RBD symptoms was investigated by retrospective interviews of the subjects and their bed partners. For this reason, we may have been unable to detect the existence of mild RBD symptoms in our subjects.

In conclusion, reduced MIBG uptake on scintigrams could be observed in PD patients with RBD symptoms. Although definitive

Table 1
Comparison of descriptive variables among the three subject groups.

	Groups with clinical RBD ($n = 18$)	Groups with subclinical RBD ($n = 8$)	Groups with Normal REM sleep ($n = 23$)	Significance
Age	71.3 ± 8.3	65.4 ± 8.6	71.5 ± 7.2	n.s.
Gender (Male/Female)	5/13	3/5	10/13	n.s.
Length of PD morbidity	9.0 ± 4.7	3.6 ± 2.6	5.3 ± 4.8	n.s.
Hoehn &Yahr Stages	3.0 ± 0.9	2.5 ± 0.5	2.7 ± 0.9	n.s.
Levodopa dose Equivalents (mg/day)	408 ± 214	283 ± 193	347 ± 199	n.s.
MMSE	25.6 ± 3.9	26.8 ± 2.3	26.3 ± 3.2	n.s.

RBD: REM sleep behavior disorders; MMSE: Mini Mental State Examination.
The values are expressed as mean ± SD. n.s.: not significant.

Please cite this article in press as: Nomura T, et al., Relationship between ^{123}I-MIBG scintigrams and REM sleep..., Parkinsonism and Related Disorders (2010), doi:10.1016/j.parkreldis.2010.08.011

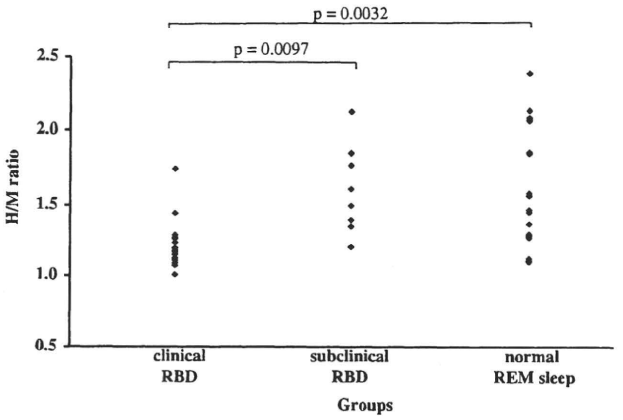

Fig. 1. Comparison of delayed image on MIBG scintigraphic findings among the three groups. ◆ symbols indicate the H/M ratios on MIBG scintigrams for each patient among the three groups (clinical RBD, subclinical RBD, and normal REM sleep).

Table 2
Multiple regression analysis on factors associated with H/M ratio on MIBG scintigrams among the total PD patients.

Model	β	t	p
Age	−0.243	−1.831	0.074
Duration of PD morbidity	0.75	0.488	0.628
Hoehn & Yahr stages	−0.104	−0.721	0.475
The existence of RBD symptoms	−0.511	−3.267	0.002
The existence of RWA on PSG	0.61	0.410	0.684

H/M: heart-to-mediastinum, MIBG: meta-iodobenzylguanidine.
RBD: REM sleep behavior disorders, RWA: REM sleep without atonia.

conclusions cannot be obtained from the results of this study, RBD symptoms might be associated with wider α-synuclein pathology as reflected by cardiac autonomic dysfunction.

Acknowledgements

We would like thank Mr. Tatsuo Kagimura of Tokyo Medical University for his generous help with the statistical analysis.

References

[1] American Academy of Sleep Medicine. International classification of sleep disorders: diagnostic and coding manual. 2nd ed.; 2005. Westchester p. 148–52.
[2] Nomura T, Inoue Y, Mitani H, Kawahara R, Miyake M, Nakashima K. Visual hallucinations as REM sleep behavior disorders in patients with Parkinson's disease. Mov Disord 2003;18:812–7.
[3] Postuma RB, Gagnon JF, Vendette M, Charland K, Montplasir JY. Manifestations of Parkinson disease differ in association with REM sleep behavior disorder. Mov Disord 2008;23:1665–72.
[4] Braune S, Reinhardt M, Schnitzer R, Riedel A, Lucking CH. Cardiac uptake of [^{123}I]MIBG separates Parkinson's disease from multiple system atrophy. Neurology 1999;53:1020–5.
[5] Miyamoto T, Miyamoto M, Inoue Y, Usui Y, Suzuki K, Hirata K. Reduced cardiac ^{123}I-MIBG scintigraphy in idiopathic REM sleep behavior disorder. Neurology 2006;67:2236–8.
[6] Uemura Y, Nomura T, Inoue Y, Yamawaki M, Yasui K, Nakashima K. Validation of the Parkinson's disease sleep scale in Japanese patients: a comparison study using the Pittsburgh sleep quality index, the Epworth sleepiness scale and polysomnography. J Neurol Sci 2009;287:36–40.
[7] American Sleep Disorders Association. Manuals of the scoring of sleep and associated events. Rules, technology, and technical specifications; 2007. p. 42–43.
[8] Oudiette M, de Cock VC, Lavault S, Leu S, Vidaihet M, Arnulf I. Nonviolent elaborate behavior may also occur in REM sleep behavior disorder. Neurology 2009;72:551–7.
[9] Hanyu H, Shimizu S, Hirao K, Sakurai H, Iwamoto T, Chikamori T, et al. The role of ^{123}I-Metaiodobenzylguanidine myocardial scintigraphy in the diagnosis of Lewy body disease in patients with Dementia in a memory clinic. Dement Geriatr Cogn Disord 2006;22:379–84.
[10] Kitayama M, Wada-Isoe K, Irizawa Y, Nakashima K. Association of visual hallucinations with reduction of MIBG cardiac uptake in Parkinson's disease. J Neurol Sci 2008;264:22–6.
[11] Ferini-Strambi L, Oldani A, Zucconi M, Smirne S. Cardiac autonomic activity during wakefulness and sleep in REM sleep behavior disorder. Sleep 1996;19:367–9.
[12] Lanfranchi PA, Fradette L, Gagnon JF, Colombo R, Montplaisir J. Cardiac autonomic regulation during sleep in idiopathic REM sleep behavior disorder. Sleep 2007;30:1019–25.

Please cite this article in press as: Nomura T, et al., Relationship between ^{123}I-MIBG scintigrams and REM sleep..., Parkinsonism and Related Disorders (2010), doi:10.1016/j.parkreldis.2010.08.011